Trajectory Tracking Control Performance Analysis of a Quadrotor in the Presence of External Disturbances

Abdurrahman Bayrak
Artificial Intelligence Department
STM Defence Inc.
Ankara, Turkey
abdurrahman.bayrak@stm.com.tr

M. Umut Demirezen
Artificial Intelligence Department
STM Defence Inc.
Ankara, Turkey
udemirezen@stm.com.tr

Mehmet Önder Efe*
Computer Engineering Department
Hacettepe University
Ankara, Turkey
onderefe@hacettepe.edu.tr

***Abstract*—This paper presents a trajectory tracking control performance analysis of some common controllers in the presence of external disturbances for Crayzflie 2.0 nano quadrotor platform. For this purpose, the mathematical model of a quadrotor and physical parameters of Crazyflie 2.0 are summarized, and LQR, PD and SMC approaches are developed for it. After that, the performances of them are investigated through simulations in the presence of matched external disturbances in the horizontal plane for a squared trajectory. Simulation results indicate that PD and LQR controllers perform satisfactory results for a certain degree of bounds based on the linearized quadrotor dynamics without any disturbance, while SMC provides more robust performance even in the presence of external disturbances for trajectory tracking.**

***Index Terms*—trajectory tracking, external disturbances, quadrotor, LQR, PD, SMC**

I. Introduction

Quadrotors have an important place for human life, because over the last decade, they have been used in many areas both civilian and military applications, such as search, surveillance, rescue, tracing, aerial photography and postal service due to their size and maneuverability. Therefore, there are a great amount of the studies about the modelling and control of the quadrotors in the literature [1], [2], [3], [4]. Despite all these efforts, the modelling and control of the quadrotors is still among the subjects which are frequently studied to make them more autonomous. What makes them so important is that they have hover, vertical take-off and landing VTOL ability and agile mobility. With these features, even complex tasks can be successfully accomplished.

Quadrotor that is an under-actuated and nonlinear coupled system, has four rotors and six degrees of freedom (6 DOF) involving the both translational and rotational dynamical equations. Its unstable nature has required many different control methods [5], [6], [7], [8]. The most remarkable control methods among them are optimal control, robust control, adaptive control and intelligent control. The main goal of these control strategies is to achieve the best performance in the quadrotor control. However, there are many factors that affect the performance of the quadrotors such as unmodelled dynamics, parameter uncertainties, all external force and moment disturbances, payload changes and sensor measurement noises during the quadrotor flights. In order to deal with these factors, many linear and non-linear controllers including above control strategies have been developed. The most commonly used among them is the Proportional Integral Derivative (PID) controller because of its simplicity, practicability and low cost. Easy parameter gain adjustment and good robustness are the main advantages of the PID controller. [9], [10], [11] are the some of the PID controller papers including position control, altitude and attitude control of the quadrotors in the literature. Although PID controller has a broad range of using, it limits the quadrotor performance because it is a linear control method and it is obtained by linearizing the quadrotor dynamic model and neglecting some factors. Therefore, it has poor performance against uncertainties and disturbances.

Another linear control method is the Linear Quadratic Regulator (LQR) algorithm that is an optimal control method. Its working principle is based on optimizing the controller gains according to a suitable cost function. [10], [12], [13] are the some of the LQR approaches on the quadrotors in the literature. Just like PID controller, it has poor performance against uncertainties and disturbances.

Sliding Mode Control (SMC) is considered as one of the robust non-linear control methods under uncertainty conditions. Like PID and LQR control, there are many studies about that in the literature [14], [15], [16], [17]. The main goal of SMC is to push the error to sliding surface and to keep the error on the close neighbourhood of the sliding surface. SMC consists of two main steps. The first one is to design a sliding surface. The second one is to design a feedback control law to keep the system on sliding surface.

In this paper, for a Crazyflie 2.0 nano quadrotor platform, PD, LQR and SMC approaches are presented and their performances are demonstrated through simulations against external disturbances in the horizontal plane.

This paper is organized as follows: In section II, the mathematical model of quadrotor and physical parameters

*Corresponding author

978-1-7281-1929-8/18/$31.00 ©2018 IEEE
DOI 10.1109/EECS.2018.00068

of Crazyflie 2.0 nano quadrotor are summarized. Section III explains the control methods. Section IV presents simulation results and discussion. Finally, the last section is devoted for conclusion.

II. The Mathematical Model of Quadrotor

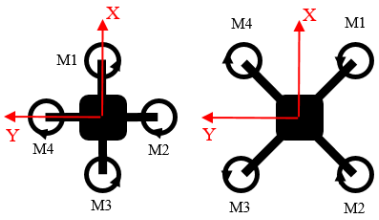

Fig. 1. Plus-configuration at the left, cross-configuration at the right.

Quadrotors have two common types of configuration as depicted in Fig. 1: Cross-Configuration and Plus-Configuration. While plus-configuration has more acrobatic structure, cross-configuration is more stable and it is usually preferred when a camera is used in the quadrotor system.

TABLE I
The Rotational Movements Comparison of Two Configurations

	PLUS-CONFIGURATION		
MOTOR	ROLL	PITCH	YAW
1	Ω_h	Ω_h - $\Delta\Omega$	Ω_h - $\Delta\Omega$
2	Ω_h - $\Delta\Omega$	Ω_h	Ω_h + $\Delta\Omega$
3	Ω_h	Ω_h + $\Delta\Omega$	Ω_h - $\Delta\Omega$
4	Ω_h + $\Delta\Omega$	Ω_h	Ω_h + $\Delta\Omega$
	CROSS-CONFIGURATION		
1	Ω_h - $\Delta\Omega$	Ω_h - $\Delta\Omega$	Ω_h - $\Delta\Omega$
2	Ω_h - $\Delta\Omega$	Ω_h + $\Delta\Omega$	Ω_h + $\Delta\Omega$
3	Ω_h + $\Delta\Omega$	Ω_h + $\Delta\Omega$	Ω_h - $\Delta\Omega$
4	Ω_h + $\Delta\Omega$	Ω_h - $\Delta\Omega$	Ω_h + $\Delta\Omega$

Table I shows the comparison of rotational movements of two configurations by considering motor propeller speeds. Where Ω_h is motor speed (RPS) required for hover.

For two configurations, vertical movement is obtained by increasing or decreasing the speed of four motor propellers equally.

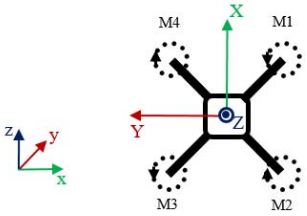

Fig. 2. Quadrotor model.

There are a lot of studies about derivation and analysis of the mathematical model of quadrotors in the literature. The full nonlinear mathematical model of a quadrotor can be summarized as follows ($cos : c$ and $sin : s$)

$$\begin{bmatrix} m\ddot{x} \\ m\ddot{y} \\ m\ddot{z} \end{bmatrix} = \begin{bmatrix} (c_\psi s_\theta c_\phi + s_\psi s_\phi)U_1 + d_x \\ (s_\psi s_\theta c_\phi - c_\psi s_\phi)U_1 + d_y \\ (c_\theta c_\phi)U_1 - mg + d_z \end{bmatrix} \tag{1}$$

$$\begin{bmatrix} I_x\dot{p} \\ I_y\dot{q} \\ I_z\dot{r} \end{bmatrix} = \begin{bmatrix} (U_2 + (I_y - I_z)qr - Jq\Omega_S) + d_\phi \\ (U_3 + (I_z - I_x)pr + Jp\Omega_S) + d_\theta \\ (U_4 + (I_x - I_y)pq) + d_\psi \end{bmatrix} \tag{2}$$

where x, y, z are the relative position of the quadrotor in inertial fram; ϕ, θ, ψ are the Euler angles related to orientation of quadrotor; namely roll-pitch-yaw angle of a quadrotor; p, q, r are the body anguler rates; m is the quadrotor mass; I is the quadrotor body inertia matrix that is assumed diagonal form in this paper; g is the acceleration of gravity; U_1 is the total lift force; U_2, U_3, U_4 are the torques acting on quadrotor; J is the moment inertia of the propellers; $\Omega_S = \Omega_2 + \Omega_4 - \Omega_1 - \Omega_3$, and finally d_i is the bounded and unknown external disturbance terms which are the force disturbances for $(i = x, y, z)$ and the moment disturbances for $(i = \phi, \theta, \psi)$.

The following equation shows the relation between the Euler angle rates and the body angular rates [2]

$$\begin{bmatrix} \dot{\phi} \\ \dot{\theta} \\ \dot{\psi} \end{bmatrix} = \begin{bmatrix} 1 & s_\phi t_\theta & c_\phi t_\theta \\ 0 & c_\phi & -s_\phi \\ 0 & \frac{s_\phi}{c_\theta} & \frac{c_\phi}{c_\theta} \end{bmatrix} \begin{bmatrix} p \\ q \\ r \end{bmatrix} \tag{3}$$

Fig. 2 shows the quadrotor model with cross-configuration used in this paper. From Fig. 2 and Table I, the total lift force U_1 and the torques acting on quadrotor can be written as differences of the thrust forces of the propellers.

$$\begin{bmatrix} U_1 \\ U_2 \\ U_3 \\ U_4 \end{bmatrix} = \begin{bmatrix} 1 & 1 & 1 & 1 \\ -\frac{l}{\sqrt{2}} & -\frac{l}{\sqrt{2}} & \frac{l}{\sqrt{2}} & \frac{l}{\sqrt{2}} \\ -\frac{l}{\sqrt{2}} & \frac{l}{\sqrt{2}} & \frac{l}{\sqrt{2}} & -\frac{l}{\sqrt{2}} \\ -\kappa & \kappa & -\kappa & \kappa \end{bmatrix} \begin{bmatrix} f_1 \\ f_2 \\ f_3 \\ f_4 \end{bmatrix} \tag{4}$$

$$\begin{aligned} f_i &= K_F \Omega_i^2 \\ \tau_i &= \kappa f_i \end{aligned} \tag{5}$$

where f_i and τ_i are the thrust and torque generated by each rotor $(i = 1, 2, 3, 4)$. Ω_i is i^{th} motor speed, K_F is a positive thrust factor, κ is translation factor between the thrust and torque and finally l is the arm length of the quadrotor.

A. Physical Parameters of Quadrotor

In this paper, Crazyflie 2.0 nano quadrocopter is used as a quadrotor platform. Table II shows the physical parameters of it. These parameters are found by using the system identification methods in [18].

As rotor dynamic model, the following first order transfer function is used.

$$\frac{\Omega(s)}{\Omega_d(s)} = \frac{1}{T_{rot}s + 1} \tag{6}$$

where T_{rot} is the time constant of the rotor dynamics. Ω_d and Ω are desired and actual rotor speed, respectively.

TABLE II
THE PHYSICAL PARAMETERS OF CRAZYFLIE 2.0 QUADROTOR PLATFORM

Symbol	Description	Value(Unit)
m	Quadrotor mass	$0.028(kg)$
l	Quadrotor arm length	$0.065(m)$
I_x	Inertial moment along x-axis	$16.571710x10^{-6}(kg.m^2)$
I_y	Inertial moment along y-axis	$16.655602x10^{-6}(kg.m^2)$
I_z	Inertial moment along z-axis	$29.261652x10^{-6}(kg.m^2)$
K_F	Thrust factor	$1.61x10^{-8}(N.s^2)$
κ	From thrust to torque factor	0.006
J	Moment inertia of propellers	0
T_{rot}	Time cons. of the rotor dyn.	0.05
Ω_{max}	Max. rotor speed	$3050(rad/sec)$
Ω_{min}	Min. rotor speed	$0(rad/sec)$
U_{1max}	Max. force	$0.71(N)$
U_{1min}	Min. force	$0.07(N)$
τ_{max}	Max. torque	$1x10^{-3}(Nm)$
τ_{min}	Min. torque	$-1x10^{-3}(Nm)$
ϕ, θ_{dmax}	Max. des. angle	$0.5(rad)$
ϕ, θ_{dmin}	Min. des. angle	$-0.5(rad)$

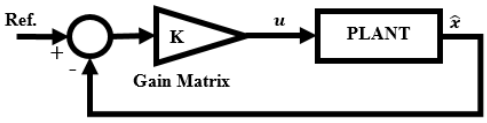

Fig. 3. LQR control scheme.

III. CONTROL METHODS

In this section, for the Crazyflie 2.0 platform, three control schemes are designed: LQR, PD and SMC. While fig. 3 shows the LQR control scheme, fig. 4 shows both SMC and PD control general block diagram.

A. LQR Control Design

LQR controller is an optimal control solution and generates a static gain matrix K based on a suitable cost function. Detailed information about LQR algorithm can be found in [10]. For this paper, to find a static gain matrix K, non-linear equations of the quadrotor are linearized and matlab **lqr** command is used. LQR controller is designed as a full state controller and applied to non-linear model of the quadrotor. In fig. 3, the input of plant consists of the motor thrusts f_1 to f_4.

$$\mathbf{u} = \begin{bmatrix} f_1 \\ f_2 \\ f_3 \\ f_4 \end{bmatrix} \tag{7}$$

$$\hat{\mathbf{x}} = \begin{bmatrix} x & y & z & \dot{x} & \dot{y} & \dot{z} & \phi & \theta & \psi & \dot{\phi} & \dot{\theta} & \dot{\psi} \end{bmatrix} \tag{8}$$

For non-linear analysis, the input of plant is as below

$$\mathbf{u} = \begin{bmatrix} f_1 \\ f_2 \\ f_3 \\ f_4 \end{bmatrix} + \begin{bmatrix} \frac{mg}{4} \\ \frac{mg}{4} \\ \frac{mg}{4} \\ \frac{mg}{4} \end{bmatrix} \tag{9}$$

B. PID Control Design

There are numerous studies about PID control in the literature. Well-known control method classical PID law is as below

$$\mathbf{u}_{pid} = K_p \mathbf{e} + K_i \int \mathbf{e} + K_d \dot{\mathbf{e}} \tag{10}$$

where $\mathbf{e} = \hat{\mathbf{x}}_{desired} - \hat{\mathbf{x}}$.

All controller blocks in fig. 4 use the above control law except the integral term. Altitude and attitude controllers produce desired force and torques, respectively. While 'OMEGA TO FORCE & TORQUES' block includes eqn. 4 and 5, 'FORCE & TORQUES TO OMEGA' block has following equations

$$\begin{bmatrix} \Omega_1^2 \\ \Omega_2^2 \\ \Omega_3^2 \\ \Omega_4^2 \end{bmatrix} = \begin{bmatrix} \frac{1}{4K_F} & -\frac{\sqrt{2}}{4K_F l} & -\frac{\sqrt{2}}{4K_F l} & -\frac{1}{4\kappa K_F} \\ \frac{1}{4K_F} & -\frac{\sqrt{2}}{4K_F l} & \frac{\sqrt{2}}{4K_F l} & \frac{1}{4\kappa K_F} \\ \frac{1}{4K_F} & \frac{\sqrt{2}}{4K_F l} & \frac{\sqrt{2}}{4K_F l} & -\frac{1}{4\kappa K_F} \\ \frac{1}{4K_F} & \frac{\sqrt{2}}{4K_F l} & -\frac{\sqrt{2}}{4K_F l} & \frac{1}{4\kappa K_F} \end{bmatrix} \begin{bmatrix} U_1 \\ U_2 \\ U_3 \\ U_4 \end{bmatrix} \tag{11}$$

$\mathbf{\Omega}_d$ is obtained by taking square root of eqn. 11.

Finally, to obtain ϕ_d and θ_d, in the position controller block, the following translation is used after PD position control law

$$\begin{bmatrix} F_x \\ F_y \\ F_z \end{bmatrix} = m. * R^{-1}(\begin{bmatrix} \ddot{x_p} \\ \ddot{y_p} \\ e_z \end{bmatrix} + \begin{bmatrix} 0 \\ 0 \\ g \end{bmatrix}) \tag{12}$$

where $\ddot{x_p}$ and $\ddot{y_p}$ are the output of the PD position control law. F_i is the desired forces in the body frame ($i = x, y, z$). R is the rotation matrix from body to inertial frame and is given with eqn. 13.

$$R = \begin{bmatrix} c\psi c\theta & c\psi s\theta s\phi - s\psi c\phi & c\psi s\theta c\phi + s\psi s\phi \\ s\psi c\theta & s\psi s\theta s\phi + c\psi c\phi & s\psi s\theta c\phi - c\psi s\phi \\ -s\theta & c\theta s\phi & c\theta c\phi \end{bmatrix} \tag{13}$$

$$\begin{bmatrix} \phi_d \\ \theta_d \end{bmatrix} = \begin{bmatrix} -arctan2(F_y, F_z) \\ arctan2(F_x, F_z) \end{bmatrix} \tag{14}$$

C. Sliding Mode Control Design

Sliding Mode Control is considered as one of the robust control methods under uncertainty conditions. The main goal of SMC is to push the error to sliding surface and to keep the error on the close neighbourhood of the sliding surface. SMC is consists of two main steps. The first one is to design a sliding surface. The second one is to design a feedback control law to keep the system on sliding surface. For this paper, sliding surface and feedback control law are selected as below

$$s = \dot{e} + \lambda e \tag{15}$$

$$u_{smc} = u_{eq} + u_D \tag{16}$$

where $u_D = ksign(s)$, λ and k are positive constant values, and u_{eq} is equivalent control term based on dynamic inversion.

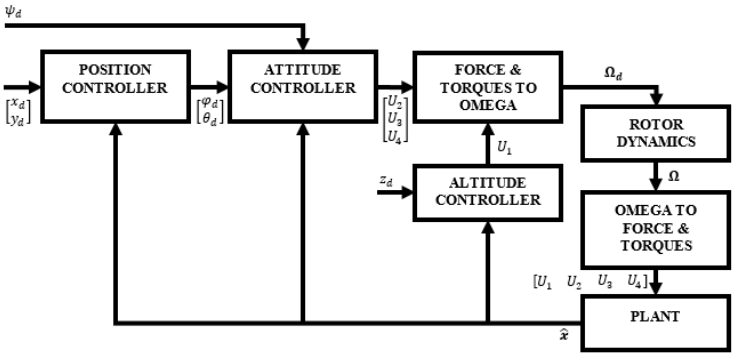

Fig. 4. Quadrotor general control scheme.

As chattering phenomena is the main disadvantage of SMC in presence of the uncertainty, u_D is taken as below

$$u_D = \frac{ks}{|s| + \epsilon} \tag{17}$$

where ϵ is positive smoothing variable preventing SMC from chattering. The force and torque smc control laws are found under $p, q, r \; = \dot{\phi}, \dot{\theta}, \dot{\psi}$ assumption as below from [14], [15].

$$U_1 = \frac{m}{c\phi c\theta}(g + \ddot{z}_{ref} + \lambda_z \dot{e}_z + \frac{k_z s_z}{|s_z| + \epsilon_z}) \tag{18}$$

$$U_2 = I_x(\ddot{\phi}_{des} + \frac{J\dot{\theta}\Omega_S}{I_x} - \frac{\dot{\theta}\dot{\psi}(I_y - I_z)}{I_x} + \lambda_\phi \dot{e}_\phi + \frac{k_\phi s_\phi}{|s_\phi| + \epsilon_\phi}) \tag{19}$$

$$U_3 = I_y(\ddot{\theta}_{des} - \frac{J\dot{\phi}\Omega_S}{I_y} - \frac{\dot{\phi}\dot{\psi}(I_z - I_x)}{I_y} + \lambda_\theta \dot{e}_\theta + \frac{k_\theta s_\theta}{|s_\theta| + \epsilon_\theta}) \tag{20}$$

$$U_4 = I_x(\ddot{\psi}_{des} - \frac{\dot{\phi}\dot{\theta}(I_x - I_y)}{I_z} + \lambda_\psi \dot{e}_\psi + \frac{k_\psi s_\psi}{|s_\psi| + \epsilon_\psi}) \tag{21}$$

For position control, eqn. 12, 13 and 14 are used.

IV. Simulation Results

In the previous sections, the mathematical model of quadrotor and control methods are explained. This section includes the simulation results. Eqn. 22, 23, 24, table III and IV show the control parameters for designed controllers.

$$K(:, 1:4) = \begin{bmatrix} -0.0157 & 0.0158 & 0.0223 & -0.0090 \\ 0.0157 & 0.0155 & 0.0223 & 0.0089 \\ 0.0156 & -0.0155 & 0.0223 & 0.0088 \\ -0.0156 & -0.0158 & 0.0223 & -0.0087 \end{bmatrix} \tag{22}$$

$$K(:, 5:8) = \begin{bmatrix} 0.0091 & 0.0177 & -0.0259 & -0.0254 \\ 0.0086 & 0.0177 & -0.0230 & 0.0249 \\ -0.0087 & 0.0177 & 0.0234 & 0.0242 \\ -0.0090 & 0.0177 & 0.0254 & -0.0237 \end{bmatrix} \tag{23}$$

$$K(:, 8:12) = \begin{bmatrix} -0.0220 & -0.0027 & -0.0025 & -0.0080 \\ 0.0224 & -0.0017 & 0.0024 & 0.0077 \\ -0.0226 & 0.0018 & 0.0021 & -0.0076 \\ 0.0222 & 0.0026 & -0.0020 & 0.0079 \end{bmatrix} \tag{24}$$

TABLE III
PD Parameters

	x	y	z	ϕ	θ	ψ
K_P	5	5	10	11	11	11
K_D	5	5	5	6	6	6

TABLE IV
SMC Parameters

	z	ϕ	θ	ψ
k	4	22	22	22
λ	4	4	4	4
ϵ	0.1	0.1	0.1	0.1

As mentioned in previous sections, LQR control gain matrix has been found for the linearized model and applied to the full nonlinear model. PD control and sliding mode control parameters have been set completely manually. Furthermore, it should be noted that all parameters of controllers are tuned as settling times will be almost the same for step reference signal and integral term of PID control law is not used for this paper.

As simulation steps, firstly, all designed controllers are tested for a square trajectory. After that, they are subjected to external disturbances in the horizontal plane, and results are investigated. As an external disturbance, moment disturbances are handled in eqn. 1 and 2 ($d_{phi}, d_{theta}, d_{psi}$). These moment

disturbances are the band limited white noise with the power $1e-9$. For all simulations, ψ_d is set to zero. Fig.5-17 indicates the simulation results.

LQR trajectory tracking results can bee seen from fig. 5-7. When compared to linear system response, LQR controller is worse in the z direction for non-linear system. In the x and y directions, LQR controller generates the same response for both systems. In presence of the external disturbances, LQR presents acceptable results except z direction. However, as LQR controller is obtained for a linear system, it has some limitations for trajectory tracking. As the boundary of trajectory increases, trajectory tracking performance decreases even under the disturbance free conditions. Therefore, for LQR analysis, 1 m^2 square trajectory is selected.

Fig.8-12 shows the PD controller trajectory tracking results. While PD controller presents good results without any disturbance for trajectory tracking, its trajectory tracking performance decreases when the disturbance applied.

In fig. 13-17, SMC trajectory tracking results are presented. When simulation results are investigated, it can be seen that SMC provides better results even in presence of external disturbance.

It can be concluded that PD and LQR provide satisfactory performance for a certain degree of bounds based on the linearized quadrotor dynamics without any disturbance, SMC provides more robust performance even in the presence of external disturbances for trajectory tracking.

Morover, it should be noted that, in eqn. 1 and 2, while d_x, d_y are the unmatched external disturbances, $d_z, d_\phi, d_\theta, d_\psi$ are the matched external disturbances [17]. In this paper, the matched external disturbances in the horizontal plane are handled. Not only LQR and PD controller, but also SMC controller can not perform well in the presence of the unmatched external disturbances for trajectory tracking [17]. To overcome from the unmatched external disturbances, a transformation (decoupling of dynamics) may be taken by considering the null-space dynamics of the state equations which are affected by the unmatched disturbances, or disturbance estimator approaches can be developed [17], [19].

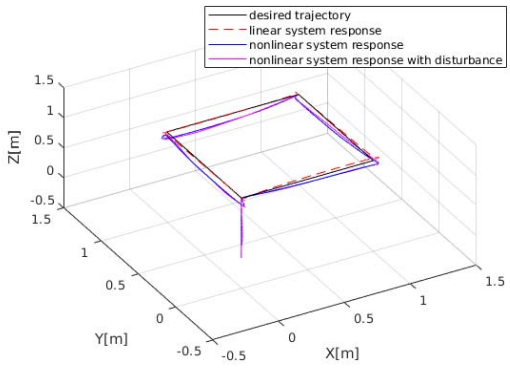

Fig. 5. LQR trajectory tracking.

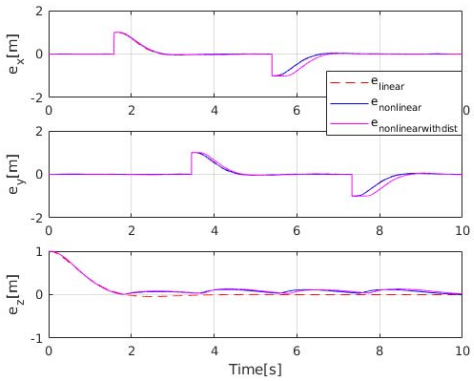

Fig. 6. LQR trajectory tracking errors.

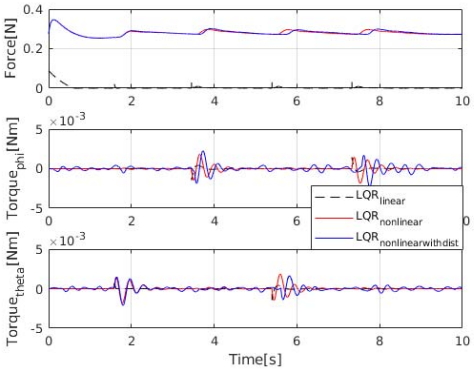

Fig. 7. LQR trajectory tracking force and torques.

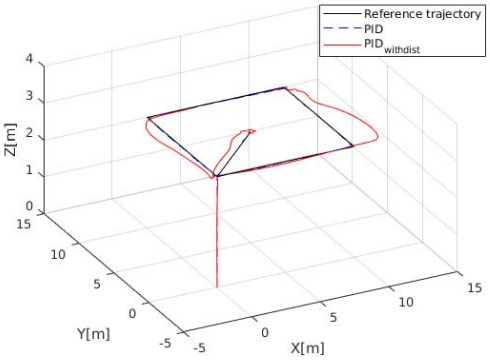

Fig. 8. PD trajectory tracking.

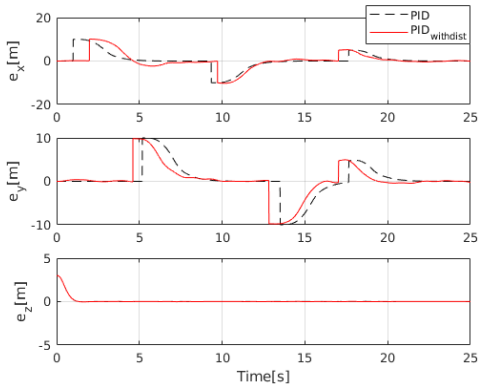

Fig. 9. PD trajectory tracking errors.

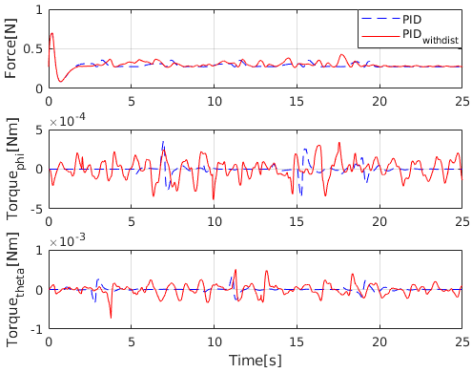

Fig. 12. PD trajectory tracking force and torques.

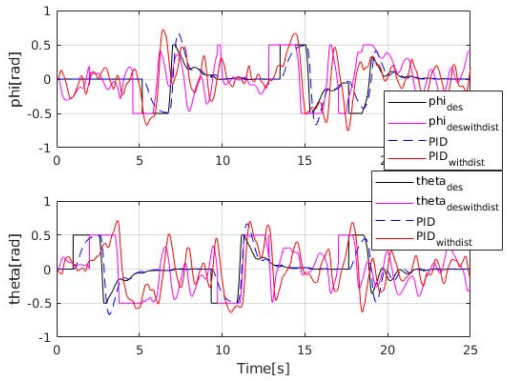

Fig. 10. Desired angles and responses for PD trajectory tracking.

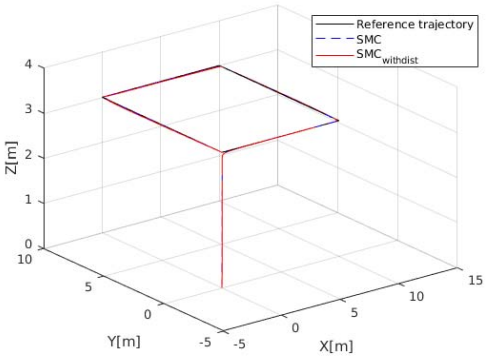

Fig. 13. SMC trajectory tracking.

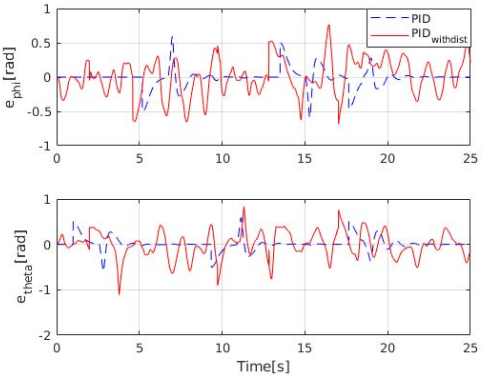

Fig. 11. Desired angles trajectory tracking errors.

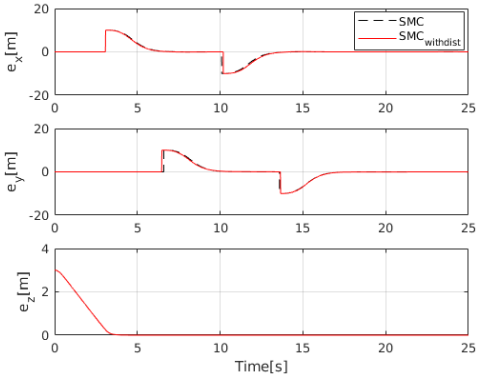

Fig. 14. SMC trajectory tracking errors.

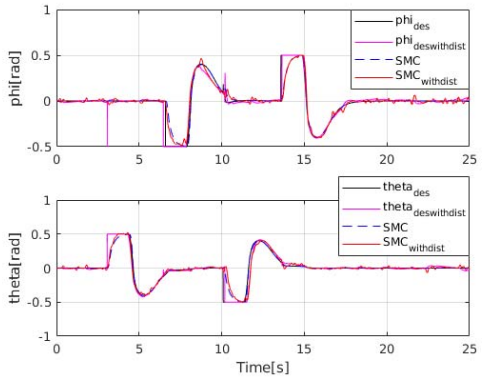

Fig. 15. Desired angles and responses for SMC trajectory tracking.

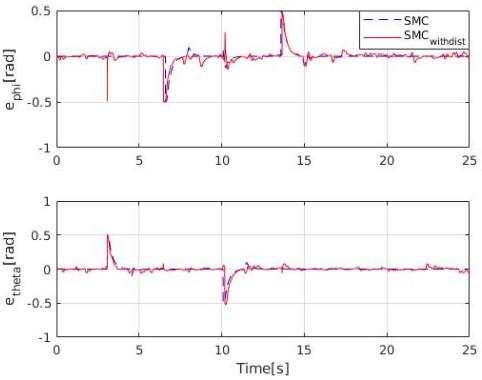

Fig. 16. Desired angles trajectory tracking errors.

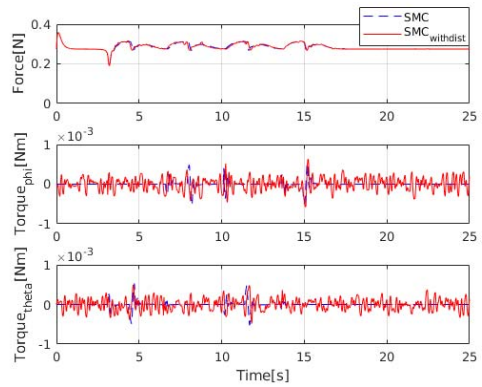

Fig. 17. SMC trajectory tracking force and torques.

V. Conclusion

In this paper, for Crayzflie 2.0 nano quadrotor platform, a trajectory tracking control performance comparison was realized against matched external disturbances. For this comdparison, LQR, PD and SMC methods were developed. Simulation results illustrate that while PD and LQR controllers provide satisfactory results in tracking accuracy for a certain degree of bounds under the nominal conditions, SMC provides very effective results both under nominal conditions and matched external uncertain disturbances.

Acknowledgment

The first author thanks TÜBİTAK BİDEB 2211-C program.

References

[1] P. Pounds, R. Mahony, P. Corke, "Modelling and control of a large quadrotor robot." Control Engineering Practice, 2010 Jul 1;18(7):691-9.
[2] T. Bresciani, "Modelling, identification and control of a quadrotor helicopter." MSc Theses, 2008.
[3] S. Bouabdallah, RY. Siegwart, "Full control of a quadrotor." InIEEE/RSJ International Conference on Intelligent Robots and Systems, 2007: IROS 2007; Oct. 29, 2007-Nov. 2, 2007, San Diego, CA 2007 (pp. 153-158).
[4] T. Luukkonen, "Modelling and control of quadcopter." Independent research project in applied mathematics, Espoo, 2011 Aug 22;22.
[5] T. Lee, M. Leok, NH. McClamroch, "Nonlinear robust tracking control of a quadrotor UAV on SE (3)." Asian Journal of Control, 2013 Mar;15(2):391-408.
[6] C. Nicol, CJ. Macnab, A. Ramirez-Serrano, "Robust adaptive control of a quadrotor helicopter." Mechatronics, 2011 Sep 1;21(6):927-38.
[7] D. Lee, HJ. Kim, S. Sastry, "Feedback linearization vs. adaptive sliding mode control for a quadrotor helicopter." International Journal of control, Automation and systems, 2009 Jun 1;7(3):419-28.
[8] GV. RRaffo, MG. Ortega, FR. Rubio, "An integral predictive/nonlinear H control structure for a quadrotor helicopter." Automatica, 2010 Jan 1;46(1):29-39.
[9] J. Li, Y. Li, "Dynamic analysis and PID control for a quadrotor." InMechatronics and Automation (ICMA), 2011 International Conference on 2011 Aug 7 (pp. 573-578).
[10] S. Bouabdallah, A. Noth, R. Siegwart, "PID vs LQ control techniques applied to an indoor micro quadrotor." InProc. of The IEEE International Conference on Intelligent Robots and Systems (IROS) 2004 (pp. 2451-2456).
[11] H. Bolandi, M. Rezaei, R. Mohsenipour, H. Nemati, SM. Smailzadeh, "Attitude control of a quadrotor with optimized PID controller." Intelligent Control and Automation, 2013 Aug 7;4(03):335.
[12] ID. Cowling, JF. Whidborne, AK. Cooke, "Optimal trajectory planning and LQR control for a quadrotor UAV." InInternational Conference on Control 2006 Aug.
[13] E. Reyes-Valeria, R. Enriquez-Caldera, S. Camacho-Lara, J. Guichard, "LQR control for a quadrotor using unit quaternions: Modeling and simulation." InElectronics, Communications and Computing (CONIELECOMP), 2013 International Conference on 2013 Mar 11 (pp. 172-178).
[14] R. Xu, U. Ozguner, "Sliding mode control of a quadrotor helicopter." InDecision and Control, 2006 45th IEEE Conference on 2006 Dec 13 (pp. 4957-4962).
[15] K. Runcharoon, V. Srichatrapimuk, "Sliding mode control of quadrotor." InTechnological Advances in Electrical, Electronics and Computer Engineering (TAEECE), 2013 International Conference on 2013 May 9 (pp. 552-557).
[16] R. Xu, U. Ozguner, "Sliding mode control of a class of underactuated systems." Automatica, 2008 Jan 1;44(1):233-41.
[17] J. Kasa, S. Stevanovi, T. illi, J. Stepani, "Robust output tracking control of a quadrotor in the presence of external disturbances." Transactions of FAMENA, 2014 Feb 13;37(4):29-42.
[18] J. Frster, "System identification of the crazyflie 2.0 nano quadrocopter." BS thesis, ETH Zurich, 2015.
[19] Y. Shtessel, C. Edwards, L. Fridman, A. Levant, "Conventional sliding mode observers." InSliding Mode Control and Observation 2014 (pp. 105-141). Birkhuser, New York, NY.